Axion - Experiment overview

Invisibles18 Workshop, Karlsruhe

C. Braggio
University of Padova and INFN

September 5, 2018

ARE WE HOMING IN ON AXIONS?

- a well motivated scenario:
  - physics case is stronger (potential cosmological and astrophysical role)
  - SUSY is failing tests at LHC, lack of WIMP detection in underground detectors
- blooming phase:
  - new detection concepts
  - commissioning of demonstrative small-scale setups
- upgrade to large scale experiments for established techniques
- $f_A \gg 10^7\,\mathrm{GeV} \Longrightarrow m_A \ll \mathrm{eV}$ "invisible" axion
  detection techniques are by no means common in particle physics

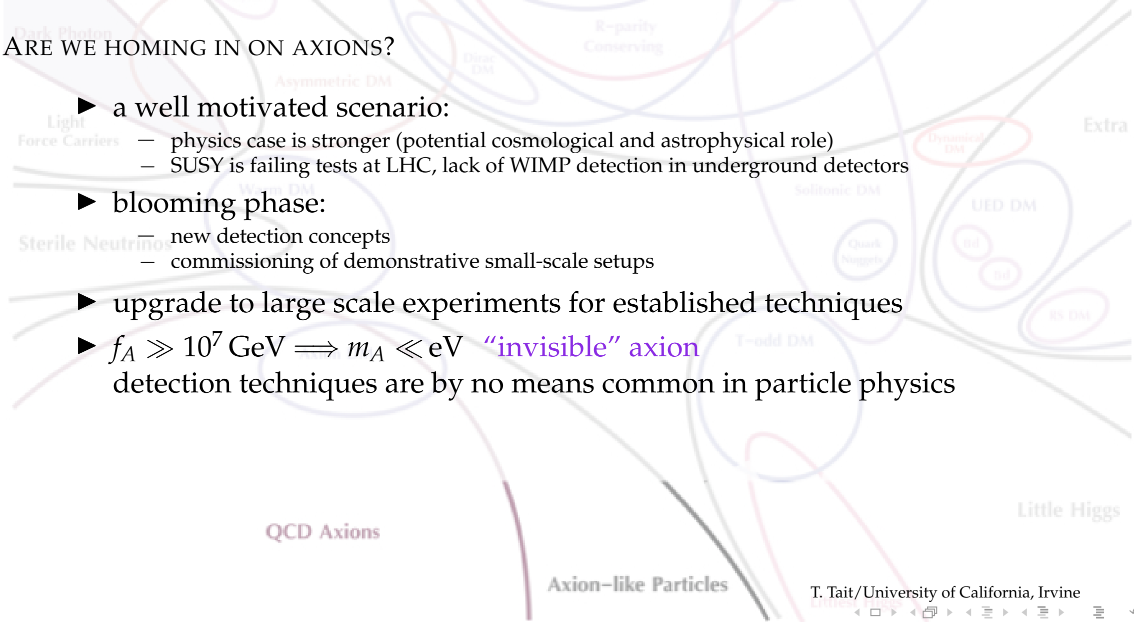

T. Tait/University of California, Irvine

AXION VS WIMP DETECTION

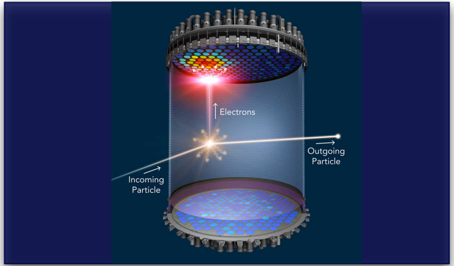

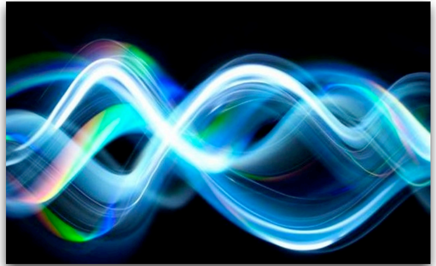

WIMP [1-100 GeV]
— number density is small
— tiny wavelength
— no detector-scale coherence

$\Longrightarrow$ observable: **scattering** of individual particles

AXION [$m_A \ll$ eV]
— number density is large (boson)
— long wavelength
— coherence within detector

$\Longrightarrow$ observable: classical, oscillating, **background field**

AXION COUPLINGS

$$\mathcal{L}_a = \frac{1}{2}\partial_\mu a\, \partial^\mu a + \frac{1}{2} m_a^2 a^2$$

An almost *model-independent axion mass*:

$$m_a \simeq 0.6 \times 10^{-4}\,\mathrm{eV} \left(\frac{10^{11}\mathrm{GeV}}{f_a} \right)$$

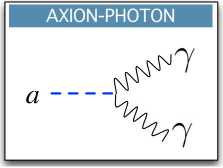

$$\mathcal{L}_{a\gamma\gamma} = -\frac{\alpha}{2\pi} f_a^{-1} g_{a\gamma\gamma}\, \mathbf{E} \cdot \mathbf{B}\, a$$

Primakoff effect:
axion detection by their decay into microwave photons in an external magnetic field **B**

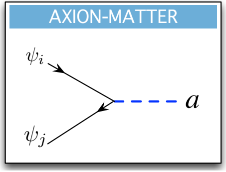

$$\mathcal{L}_a = f_a^{-1} g_{aij} \bar{\psi}_i \gamma^\mu \gamma^5 \psi_j \partial_\mu a$$

In DFSZ axion models couplings with fermions are not suppressed at tree level

SENSITIVITY PLOTS:

WE WANT TO MEASURE A MASS AND A COUPLING

Each interaction is modeled through a related coupling

- axion-photon ($g_{a\gamma}$)
- axion-electron (g_{ae})
- axion-nulceon (g_{aN})

(not straightforward to relate one coupling to another)

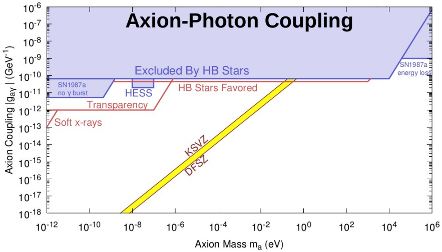

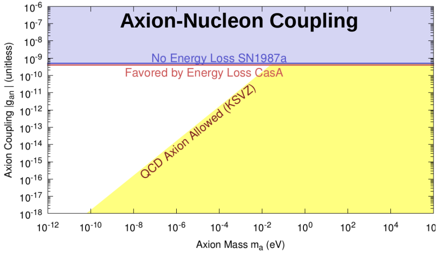

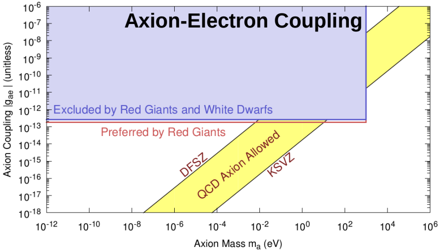

HINTS, CONSTRAINTS AND MODELS

DETECTION STRATEGIES FROM ASTROPHYSICS AND COSMOLOGY

- axions modify stellar evolution/dynamics
- axions modify intergalactic γ-ray transparency

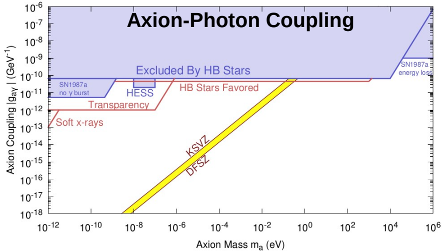

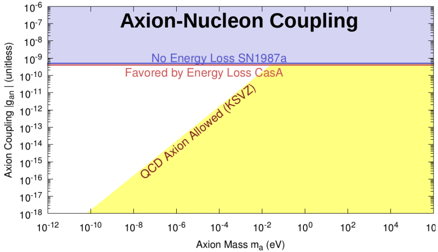

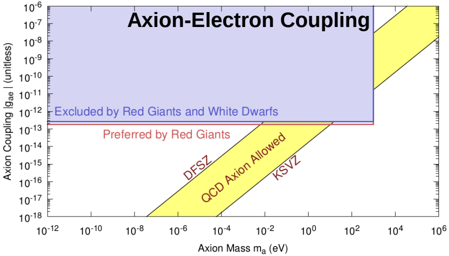

What we know about the CDM LOCAL distribution

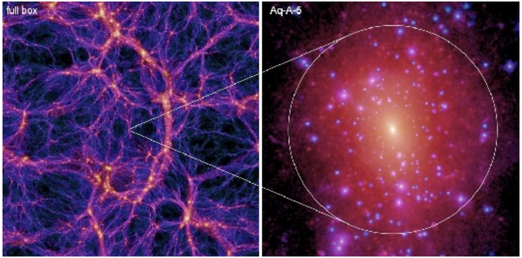

Aquarius simulation http://wwwmpa.mpa-garching.mpg.de/aquarius/
J. I. Read, The local dark matter density, J. of Phys. G 41 vol 6 (2014)

DM can have additional structures on small scales:
— if axions continuously fall into galaxies they would form caustic rings [Sikivie 2011]
— if axion DM density is dominated by few local streams, its velocity distribution can be very narrow (orders of magnitude)

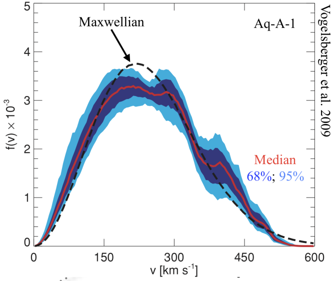

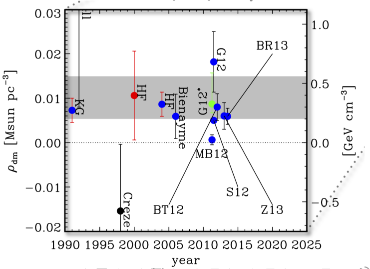

STANDARD HALO MODEL FOR ρ_{DM} AND $f(v)$

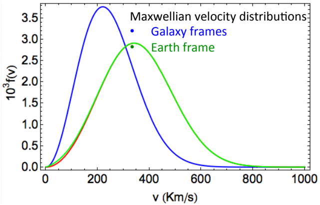

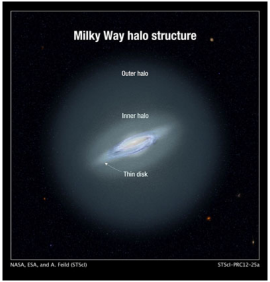

- cosmic axion density $\rho_{\mathrm{DM}} \sim 0.3\,\mathrm{GeV/cm^3}$ $[\tilde{\rho} = 1] \longrightarrow n_a \sim 3 \times 10^{12}\ (10^{-4}\ \mathrm{eV}/m_a)\ \mathrm{a/cm^3}$
- axion velocities are distributed according to a Maxwellian distribution $f(v) = 4\pi \left(\frac{\beta}{\pi}\right)^{3/2} v^2 \exp(-\beta v^2)$, with $\beta = \frac{3}{2\sigma_v^2}$, σ_v velocity dispersion
- $\sigma_v \sim 10^{-3} \rightarrow$ the axion energy distribution is monochromatic 1 part in 10^6
- + motion of E in the galaxy $\longrightarrow$ they can be seen as a wind with $v \sim 10^{-3}\,c$

MATCHING TO THE AXION LINEWIDTH

When bosons with $m_a < 10$ eV make up a significant fraction of the DM energy density (hp: all), their number density is so large that there are many of them per De Broglie wavelength volume. When that happens, their superposition can be described as a classical field oscillating at a frequency set by their mass, and a coherence time determined by the inverse energy spread $\sim 10^6$ periods of oscillation $\Longrightarrow$ *macroscopic spatial coherence*

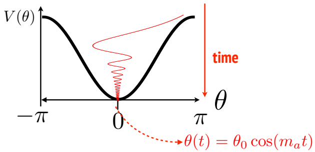

a_0 is a very small number ($B_a \sim 10^{-21}$ T) but coherent oscillations allow for detection

COHERENCE TIME

$$\tau_{\nabla a} = 0.68\tau_a \simeq 34\,\mu\text{s}\left(\frac{10^{-4}\text{eV}}{m_a}\right)$$

CORRELATION LENGTH

$$\lambda_{\nabla a} = 0.74\lambda_a \simeq 10.2\,\text{m}\left(\frac{10^{-4}\text{eV}}{m_a}\right)$$

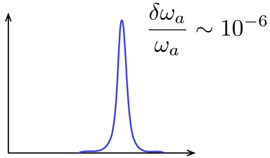

- relaxation time of the magnetized materials/lifetime of the involved atomic levels must not exceed the coherence time
- huge number of channels

THE RESONANTLY ENHANCED AXION-PHOTON CONVERSION

Pierre Sikivie

If axions are *almost monochromatic* then their conversion to detectable particles (photons) can be accomplished using *high-Q* microwave cavities.

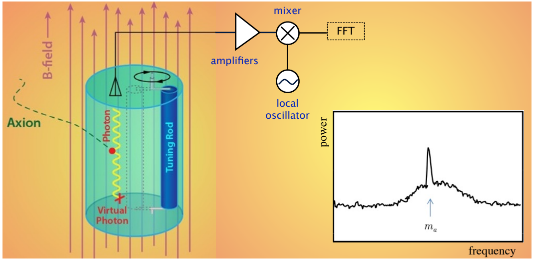

- $\omega_{\mathrm{TM}onl} = \sqrt{\left(\frac{\epsilon_n}{r}\right)^2 + \left(\frac{l\pi}{h}\right)}$ for a cylindrical cavity in a solenoidal field, the TM_{onl} are the cavity modes that couple with the axion
- resonant amplification in $[m_a \pm m_a/Q]$
- data in thin slices of parameter space (tuning rod); typically $Q < Q_a \sim 1/\sigma_v^2 \sim 10^6$

THE RESONANTLY ENHANCED AXION-PHOTON CONVERSION

PRIMAKOFF EFFECT

In a magnetic field, an axion is equivalent to a photon

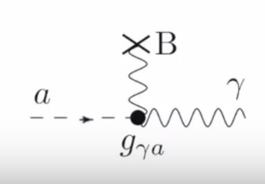

The resonantly enhanced axion-photon conversion

Signal power in the band $[m_a \pm m_a/Q]$:

$$\begin{aligned} P_s &= \kappa \frac{Q}{m_a} g_{a\gamma}^2 B_e^2 |\mathcal{G}_m|^2 V \varrho_a \\ &= 7.2 \times 10^{-23}\mathrm{W} \left(\frac{\kappa}{0.5}\right) \left(\frac{Q}{10^5}\right) \left(\frac{\mu\mathrm{eV}}{m_a}\right) \left(\frac{g_{a\gamma}}{2 \times 10^{-16}\mathrm{GeV}^{-1}}\right)^2 \left(\frac{B_e}{8\mathrm{T}}\right)^2 \left(\frac{|\mathcal{G}_m|^2}{0.69}\right) \frac{V}{200\mathrm{l}} \tilde{\varrho}_a \end{aligned}$$

THE RESONANTLY ENHANCED AXION-PHOTON CONVERSION

Signal power in the band $[m_a \pm m_a/Q]$:

$$\begin{aligned} P_s &= \kappa \frac{Q}{m_a} g_{a\gamma}^2 B_e^2 |\mathcal{G}_m|^2 V \varrho_a \\ &= 7.2 \times 10^{-23}\mathrm{W} \left(\frac{\kappa}{0.5}\right)\left(\frac{Q}{10^5}\right)\left(\frac{\mu\mathrm{eV}}{m_a}\right)\left(\frac{g_{a\gamma}}{2\times 10^{-16}\mathrm{GeV}^{-1}}\right)^2\left(\frac{B_e}{8\mathrm{T}}\right)^2\left(\frac{|\mathcal{G}_m|^2}{0.69}\right)\frac{V}{200\mathrm{l}}\tilde{\varrho}_a \end{aligned}$$

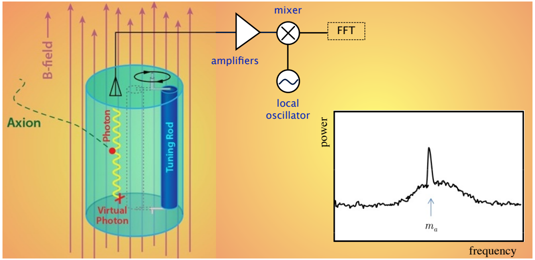

- for QCD axions, the signal is typically much smaller than noise

$$\begin{aligned} P_n &= T_{sys}\Delta\nu = T_{sys}\frac{m_a}{2\pi Q_a} \\ &= 3.3\times 10^{-21}\left(\frac{T_{sys}}{K}\right)\left(\frac{m_a}{\mu\mathrm{eV}}\right)\left(\frac{10^6}{Q_a}\right) \end{aligned}$$

  $\rightarrow$ measurement time Δt is such that $S > N$
- low noise microwave amplifiers
- **quantum sensing (below SQL)**: photon counting techniques can accelerate searches by orders of magnitude for $\nu > 10\,\mathrm{GHz}$ for $T < 100\,\mathrm{mK}$

ADMX - Washington

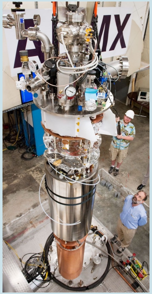

– after > 30 y of R&D,
reached sensitivity to DFSZ models
– 100 mK, SQUID
– thin slice around 2.75 μ eV
– no new technology up to 10 μ eV

PRL **120**, 151301 (2018)

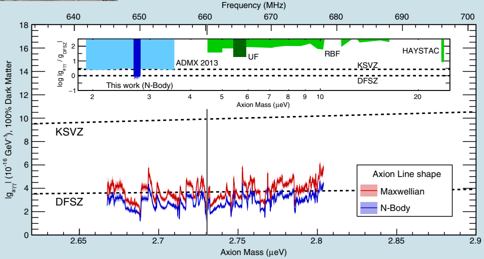

HAYSTAC - Yale

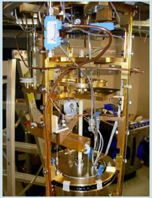

– 127 mK, JPA
– first results in a new mass range
(24 μeV)
– pushing to higher mass values

PRL **118**, 061302 (2018)

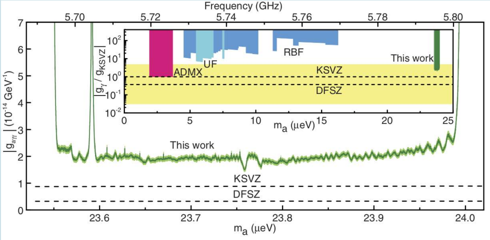

WHAT ABOUT DIFFERENT MASS RANGES?

In the conventional haloscope the effective volume falls off rapidly with increasing frequency + lower masses limitations (B field)

some non-conventional **axion detection strategies** and **complementarity** [different mass ranges, different interactions]

with a focus on recently proposed **haloscopes**

AXION-PHOTON COUPLING

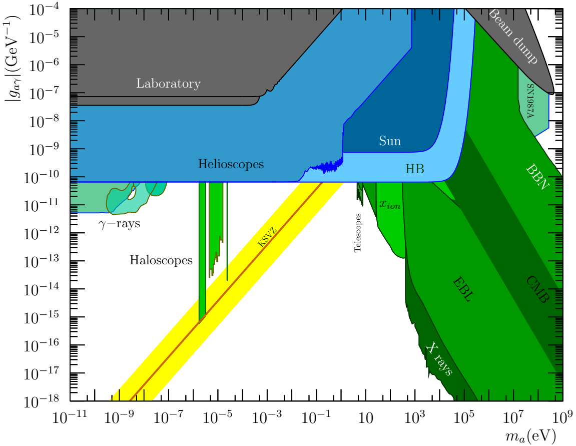

- entirely lab experiments (LSW, POL, 5$^{\text{th}}$ force)
- helioscopes, stellar astrophysics
- haloscopes/cosmology dependent
- QCD axion allowed

from I.G. Irastorza and J. Redondo, arXiv:1801.08127v2 [hep-ph]

HALOSCOPES: DEMONSTRATORS AND NEW PROPOSALS

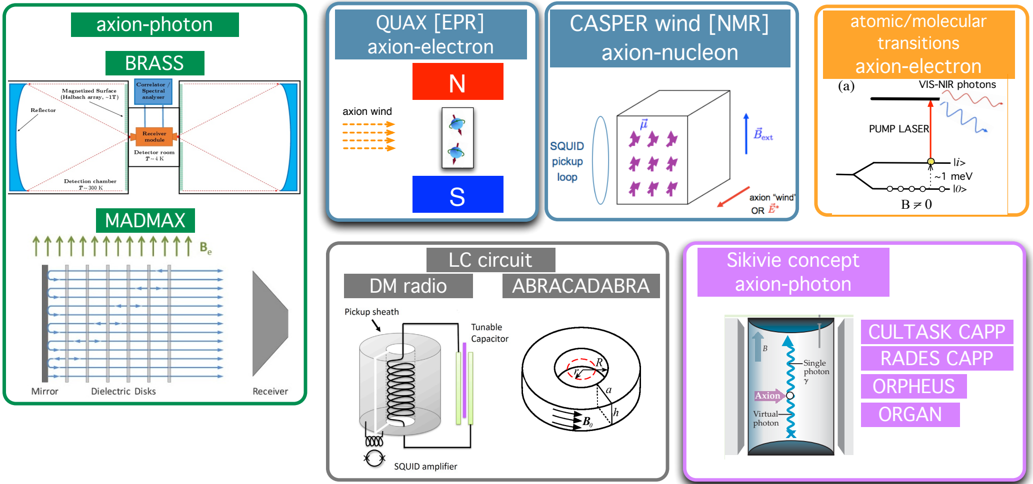

NOTE: this is just a selection. . .

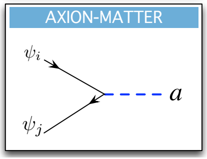

$$\mathcal{L}_a = f_a^{-1} g_{aij} \bar{\psi}_i \gamma^\mu \gamma^5 \psi_j \partial_\mu a$$

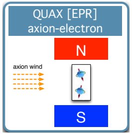

The interaction term has the form of a spin−magnetic field interaction with ∇a playing the role of a

oscillating effective magnetic field

$$i\hbar \frac{\partial \varphi}{\partial t} = \left[-\frac{\hbar^2}{2m} \nabla^2 - \frac{g_p \hbar}{2m} \boldsymbol{\sigma} \cdot \boldsymbol{\nabla} a \right] \varphi$$

$$-\frac{g_p \hbar}{2m} \boldsymbol{\sigma} \cdot \boldsymbol{\nabla} a \equiv -2 \frac{e\hbar}{2m} \boldsymbol{\sigma} \cdot \left(\frac{g_p}{2e} \right) \boldsymbol{\nabla} a$$

$-2\mu_B \boldsymbol{\sigma}$,

μ_B the Bohr magneton

$$B_a \equiv \frac{g_p}{2e} \boldsymbol{\nabla} a$$

effective magnetic field

$$\frac{\omega_a}{2\pi} = f_a = \frac{m_a c^2}{h} \simeq 14 \left(\frac{m_a}{58.5\,\mu\text{eV}} \right) \text{GHz},$$

$$B_a = \frac{g_{aee}}{2e} \sqrt{\frac{\hbar n_a}{m_a c}}\, m_a v_a$$

$$= 7 \times 10^{-23} \left(\frac{\rho_{\text{dm}}}{0.45\,\text{GeV}} \right)^{\frac{1}{2}} \left(\frac{m_a}{58.5\,\mu\text{eV}} \right) \left(\frac{v_a}{220\,\text{km/s}} \right) \text{T}$$

AXION DETECTION BY RESONANT INTERACTION WITH e^- SPIN

The interaction term has the form of a spin—magnetic field interaction with ∇a playing the role of a

oscillating effective magnetic field

$$\frac{\omega_a}{2\pi} = f_a = \frac{m_a c^2}{h} \simeq 14 \left(\frac{m_a}{58.5\,\mu\text{eV}}\right) \text{GHz},$$

$$B_a = \frac{g_{aee}}{2e} \sqrt{\frac{\hbar n_a}{m_a c}} m_a v_a$$

$$= 7 \times 10^{-23} \left(\frac{\rho_{\text{dm}}}{0.45\,\text{GeV}}\right)^{\frac{1}{2}} \left(\frac{m_a}{58.5\,\mu\text{eV}}\right) \left(\frac{v_a}{220\,\text{km/s}}\right) \text{T}$$

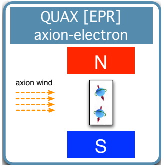

EPR/FMR technique

— By placing a ferrimagnetic sample in a static magnetic field $\mathbf{B}$ ($\perp$ axion wind) it is possible to tune the Larmor frequency of the electrons to the axion frequency ν_a (spin σ is along the z axis).

— B_a deposits in the sample the power $P_a = B_a \frac{dM}{dt} V_s = 4\pi\gamma\mu_B\nu_a B_a^2 \tau_{\min} n_s V_s$

— P_a gives rise to RF/μwave radiation $\Longleftarrow$ **axion signal**

RADIATION DAMPING

The dynamics of the magnetic sample is well described by its magnetization M, whose evolution is given by the Bloch equations. The damping term affects the **maximum allowed coherence** hence the integration time of the magnetic system with respect to the axion driving input P_a.
$\Longrightarrow$ **strong coupling regime (hybrid photon-magnon mode)**

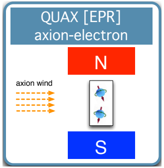

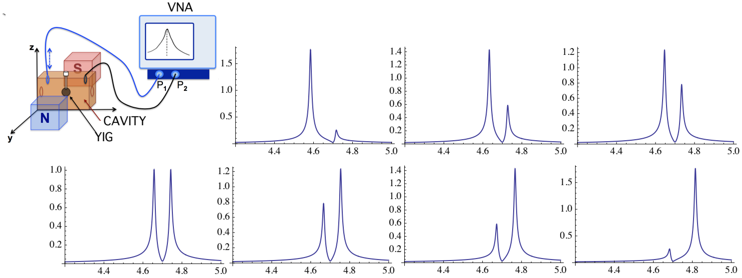

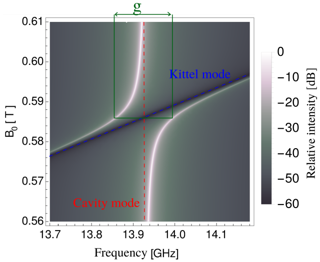

EXPERIMENTAL CHALLENGES

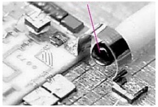

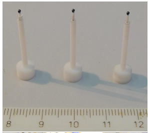

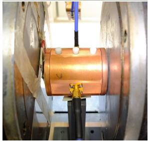

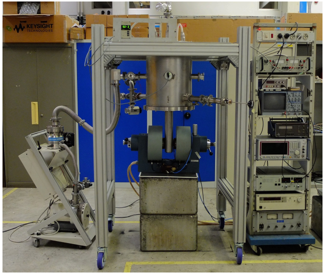

- magnetized material with spin density $2 \times 10^{28}\,\mathrm{m}^{-3}$ and FMR linewidth $\sim 150\,\mathrm{kHz}$ ($\tau_2 \sim 2\,\mu\mathrm{s}$)
- necessary magnetized sample volume $\sim 100\,\mathrm{cm}^3$ to be hosted in $\sim$ 50 GHz frequency cavities
- $\sim 10^6$ Q-factor cavity/cavities
- ppm level uniformity and high stability of the 2 T magnetic field
- signal detection beyond SQL with linear amplifiers $\Longrightarrow$ single-photon microwave detectors
- 100 mK working temperature of the complete apparatus
- frequency tunability

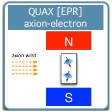

QUAX DEMONSTRATOR

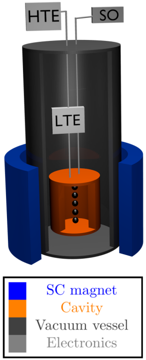

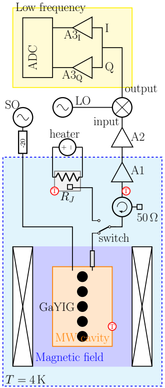

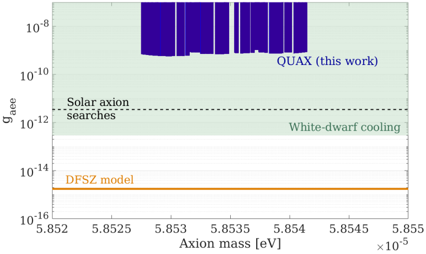

five 1-mm YIG spheres (V_s =2.6 mm^3)
HEMT low noise cryogenic amplifier

— minimum measured value of
$g_{aee} = 4.9 \times 10^{-10} \Longleftrightarrow B_a < 1.6 \times 10^{-17}$ T

GOAL: $10^{3 \div 4}$ sensitivity improvement

→ increasing the signal $V_s \sim 0.1$ liter $P_a \sim 10^{-27}$ W
→ reducing the noise [quantum counter]

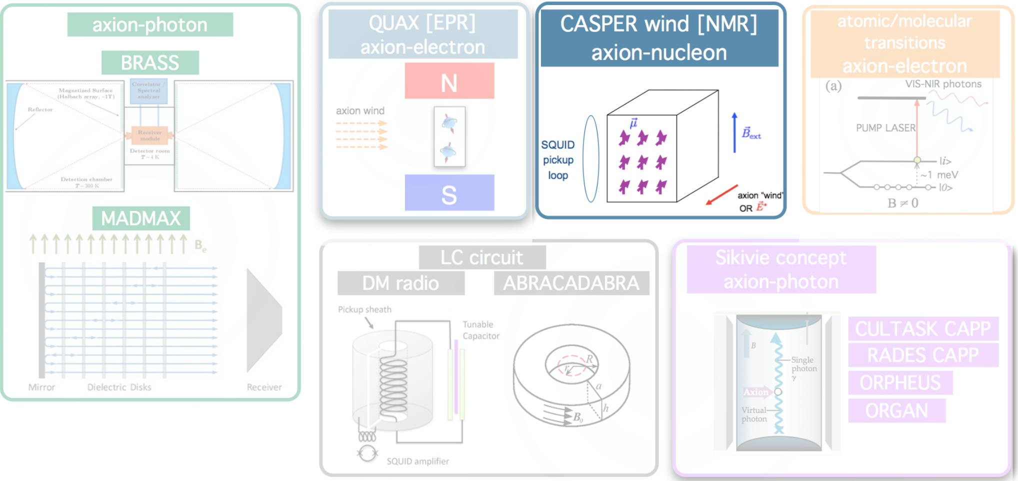
axion-photon
BRASS
Magnetized Surface (Halbach array, ~1T)
Correlator / Spectral analyser
Reflector
Receiver module
Detector room T~4 K
Detection chamber T~300 K
MADMAX
Mirror
Dielectric Disks
Receiver
QUAX [EPR]
axion-electron
N
S
axion wind
CASPER wind [NMR]
axion-nucleon
SQUID pickup loop
axion "wind" OR E*
atomic/molecular transitions
axion-electron
(a)
VIS-NIR photons
PUMP LASER
|i>
~1 meV
|0>
B ≠ 0
LC circuit
DM radio
ABRACADABRA
Pickup sheath
Tunable Capacitor
SQUID amplifier
Sikivie concept
axion-photon
Single photon
Axion
Virtual photon
CULTASK CAPP
RADES CAPP
ORPHEUS
ORGAN

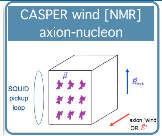

∇a couples to the relativistic fermion spin as an effective magnetic field B_a that can be searched with magnetic resonance experiments

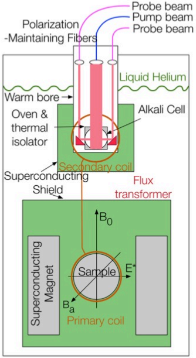

media: Xe, 3He
- can be completely polarized
- $t_2 \sim 1000\,s$ coherence time
- low frequency [no radiation damping!]
- $m_N/m_e = 2000$ [much smaller ALP masses vs QUAX]

PROSPECTED SENSITIVITY

⋆ phase I [1 cm^3 sample]

⋆ three ranges of B_e:

(0.1-14) T $\rightarrow m_a \sim$ neV$\div\mu$eV

$(10^{-4} - 0.1)$ T $\rightarrow m_a \sim$ peV$\div$neV and $B_e < 10^{-4}$ (ZULF)

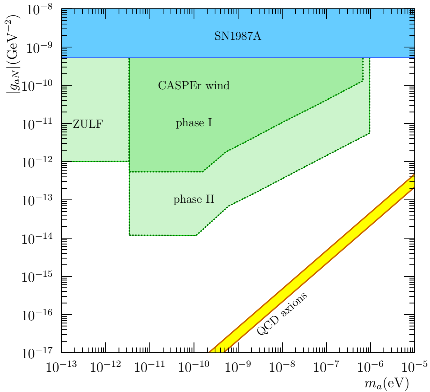

axion DM field $\equiv$ oscillating EDMs

$\theta(t) \sim \theta_0 + \theta_{\approx} \cos(m_A t)$, $\quad \theta_{\approx} \sim 4 \times 10^{-19}$ fixed by $\tilde{\rho}_A$

– p and n have EDMs $\propto \theta \implies$ their EDMs trace the axion DM oscillations: $d_n(t) \simeq 0.0024 \times \theta_{\approx} \cos(\omega t)$ e fm.

DETECTION STRATEGY: a useful analogy

the ferroelectric material displays *intrinsic* electric fields E_{int} at the nucleus position

$d_n(t) \cdot E_{\text{int}} \Longleftrightarrow \mu_N B_{\perp}(t)$

i.e. the interaction of the induced nEDM with E_{int} is equivalent to the interaction of the spin with an oscillating B-field transverse to B_e ($B_{\perp}(t)$)

CASPEr-Electric

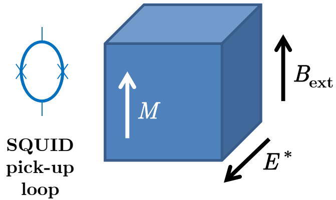

axion DM field $\equiv$ oscillating EDMs

$\theta(t) \sim \theta_0 + \theta_{\approx} \cos(m_A t)$, $\theta_{\approx} \sim 4 \times 10^{-19}$ fixed by $\tilde{\rho}_A$
– p and n have EDMs $\propto \theta \Longrightarrow$ their EDMs trace the axion DM oscillations: $d_n(t) \simeq 0.0024 \times \theta_{\approx} \cos(\omega t)$ e fm.

DETECTION STRATEGY: a useful analogy

the ferroelectric material displays *intrinsic* electric fields E_{int} at the nucleus position

$d_n(t) \cdot E_{\text{int}} \Longleftrightarrow \mu_N B_{\perp}(t)$

i.e. the interaction of the induced nEDM with E_{int} is equivalent to the interaction of the spin with an oscillating B-field transverse to B_e ($B_{\perp}(t)$)

$\Longrightarrow$ a resonant increase of the transverse magnetization when $B_{\perp}(t)$ oscillates at a frequency matching ω_L is expected!

CASPEr-Electric

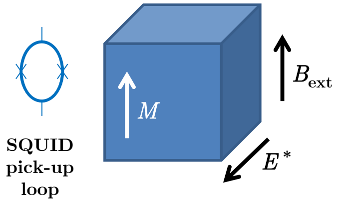

$$M_{\perp} \simeq p n_N \mu_N |d_n| E_{\text{int}} t$$

axion DM field $\equiv$ oscillating EDMs

$\theta(t) \sim \theta_0 + \theta_{\approx} \cos(m_A t)$, $\quad \theta_{\approx} \sim 4 \times 10^{-19}$ fixed by $\tilde{\rho}_A$
– p and n have EDMs $\propto \theta \implies$ their EDMs trace the axion DM oscillations: $d_n(t) \simeq 0.0024 \times \theta_{\approx} \cos(\omega t)$ e fm.

DETECTION STRATEGY: a useful analogy

the molecules are polarized so as to develop large *intrinsic* electric fields $E_{\rm int}$ at the nucleus position

$$d_n(t) \cdot E_{\rm int} \iff \mu_N B_\perp(t)$$

i.e. the interaction of the induced nEDM with $E_{\rm int}$ is equivalent to the interaction of the spin with an oscillating B-field transverse to B_e ($B_\perp(t)$)

$\implies$ a resonant increase of the transverse magnetization when $B_\perp(t)$ oscillates at a frequency matching ω_L is expected!

PROSPECTED SENSITIVITY

⋆ phase I [^{207}Pb nuclear spins in PMN-PT sample]
⋆ phase II and III [sensitivity to QCD axion m_a <neV]

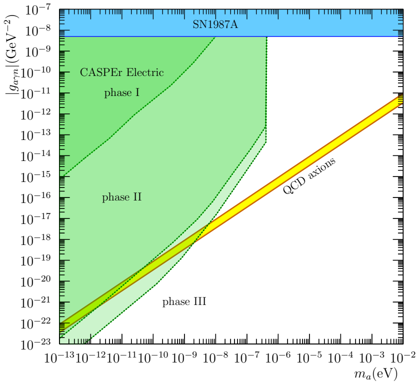

$$M_\perp \simeq p n_N \mu_N |d_n| E_{\rm int} t$$

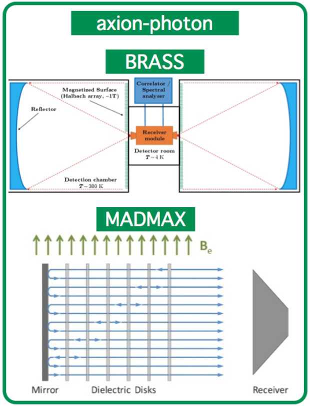
axion-photon
BRASS
Magnetized Surface (Halbach array, ~1T)
Correlator / Spectral analyser
Reflector
Receiver module
Detector room $T\sim4$ K
Detection chamber $T\sim300$ K
MADMAX
B_e
Mirror
Dielectric Disks
Receiver

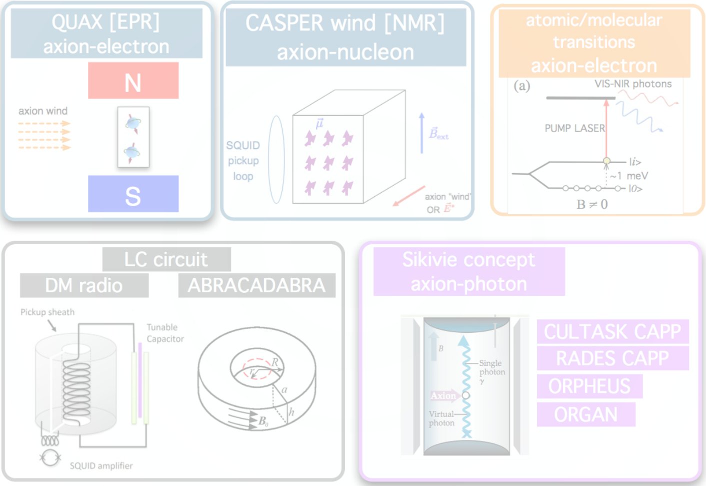
QUAX [EPR]
axion-electron
N
axion wind
S
CASPER wind [NMR]
axion-nucleon
SQUID pickup loop
$\vec{B}_{ext}$
axion "wind" OR $\vec{E}^*$
atomic/molecular transitions
axion-electron
(a)
VIS-NIR photons
PUMP LASER
|i>
~1 meV
|0>
$B \neq 0$
LC circuit
DM radio
ABRACADABRA
Pickup sheath
Tunable Capacitor
SQUID amplifier
Sikivie concept
axion-photon
CULTASK CAPP
RADES CAPP
ORPHEUS
ORGAN
B
Single photon
Axion
Virtual photon

SEARCHING THE AXION AT HIGHER MASSES

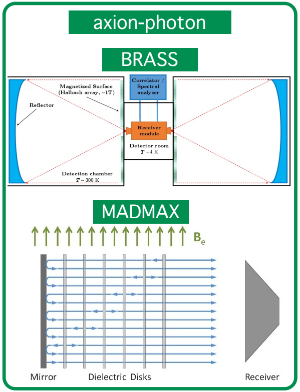

Broadband Radiometric Axion SearcheS

dish antenna concept: photons are emitted by reflective/refractive surfaces in a magnetic field B_e and the DM halo field B_a

$$E_a = \frac{g_{a\gamma} B_e\, a(t)}{\varepsilon}$$

ALP field in a medium with dielectric constant ε

$\rightarrow$ to satisfy the continuity conditions at a boundary, the pure ALP-like wave goes with photon-like waves

$$\frac{P_{\text{dish}}}{P_{\text{haloscope}}} \propto \frac{m_a^2 \mathcal{A}}{Q}$$

a dish with a magnetized area of $\mathcal{A} \sim 1\,\text{m}^2$ competes with an $Q \sim Q_a \sim 10^6$ haloscope at $m_a \sim 200\,\mu$eV

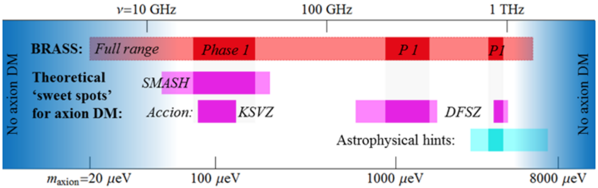

SEARCHING THE AXION AT HIGHER MASSES

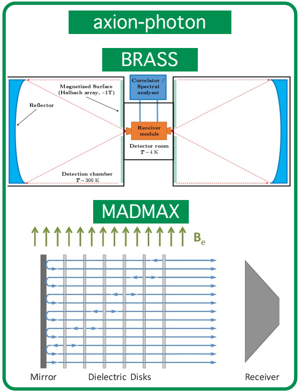

In MADMAX a boost factor N_d^2 is considered

N_d number of dielectric disks

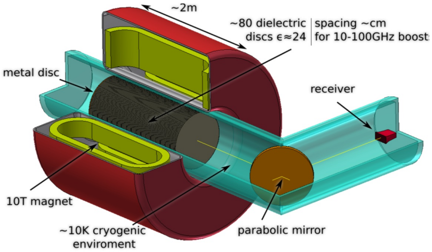

by adjusting the distances between the layers, the frequency dependence of the boosted sensitivity can be adjusted to different bandwidths

Magnetized Disc and Mirror Axion Experiment

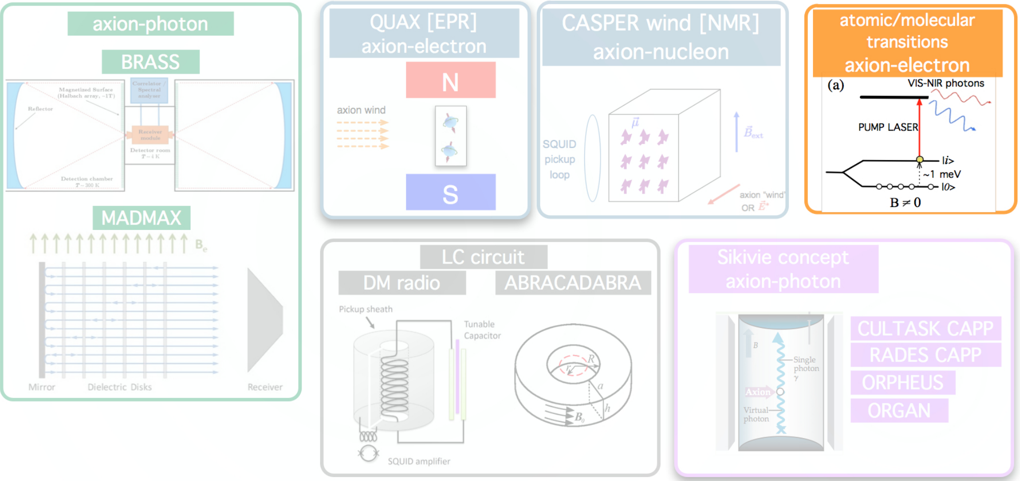

axion-photon
BRASS
MADMAX
Mirror
Dielectric Disks
Receiver
QUAX [EPR]
axion-electron
N
S
axion wind
CASPER wind [NMR]
axion-nucleon
SQUID
pickup
loop
atomic/molecular
transitions
axion-electron
(a)
VIS-NIR photons
PUMP LASER
|i>
~1 meV
|0>
B ≠ 0
LC circuit
DM radio
ABRACADABRA
Pickup sheath
Tunable
Capacitor
SQUID amplifier
Sikivie concept
axion-photon
CULTASK CAPP
RADES CAPP
ORPHEUS
ORGAN

AXION DETECTION WITH ATOMIC TRANSITIONS

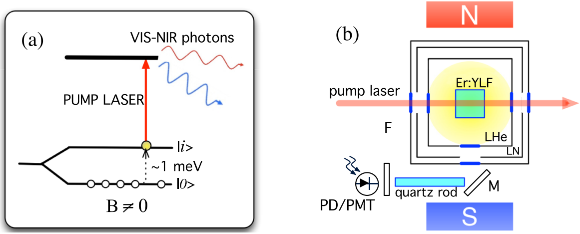

- axion-induced transitions take place between Zeeman-split ground state levels in rare-earth doped materials
- transitions involve electrons in the 4*f* shell (as if they were free atoms. . .)
- a tunable laser pumps the excited atoms to a fluorescent level
- crystal immersed in LHe and superfluid He

AXION DETECTION IN RE-DOPED MATERIALS

For one mole of target atoms (RE-dopant) in the ground state $|0\rangle$, the transition rate to the level $|i\rangle$ by axion absorption on resonance (P. Sikivie PRL (2016))

$$N_A R_i = 8.5 \times 10^{-3} \left(\frac{\rho_a}{0.4\,\mathrm{GeV/cm^3}}\right)\left(\frac{E_a}{330\,\mu\mathrm{eV}}\right)^2 g_i^2 \left(\frac{\overline{v^2}}{10^{-6} c^2}\right)\left(\frac{\min(t, \tau, \tau_{\nabla a})}{10^{-6}\,\mathrm{s}}\right)\,\mathrm{Hz}$$

where R_i is the transition rate of a single target atom, N_A is the Avogadro number, $E_a = h\nu_a$ is the axion energy

→ spectroscopic properties at "high" RE concentration (0.1 %, i.e. $\geqslant 10^{19}$ *axion target electrons*/cm^3) in ~ 1 l- active volume

the linewidth of the transition driven by the laser must be narrower than the energy difference between the atomic levels $|0\rangle$ and $|i\rangle$

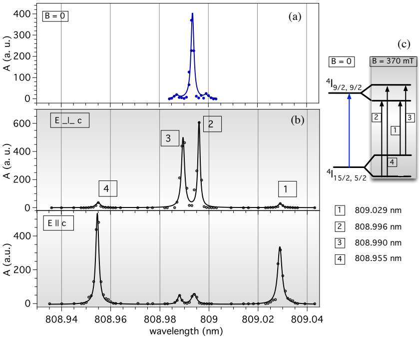

AXION DETECTION IN RE-DOPED MATERIALS: WORKING T

Thermal occupation of the Zeeman upper level needs to be suppressed

fundamental noise limit → thermal excitation of the Zeeman excited level

$$N_A R_t = \bar{n}/\tau$$

$\bar{n} = N_A \exp(-E_a/kT)$ average number of excited ions in the energy level E_a
SNR= 3, statistically significant number of counts within $t_m = 1\,\mathrm{h}$
→ thermal excitation rate $R_t = 6 \times 10^{-3}\,\mathrm{Hz}$

$\tau = 1\,\mathrm{ms}$ level lifetime → $\bar{n} \leqslant 5 \cdot 10^{-6}$

Axions with mass greater than 80 GHz can be searched, provided $T \leqslant 57\,\mathrm{mK}$.

$\Longrightarrow$ ultra-cryogenic ($T \sim 100\,\mathrm{mK}$) optical apparatus
Laser-related backgrounds ($\sim 10\,\mathrm{W/cm^2}$)?

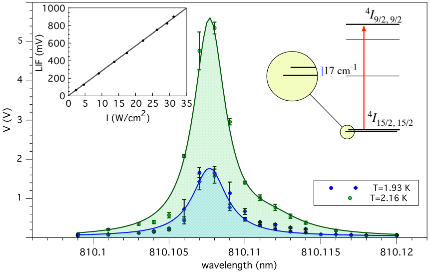

The pump laser does not affect the thermal population of the Zeeman excited level [up to a $\sim\mathrm{W/cm^2}$ intensity]

AXION DETECTION STRATEGIES: THERE'S MUCH MORE!

- DM HALOSCOPES: interaction of axions forming DM Galactic halo with SM elementary particles (photons, nuclei, and electrons)
  - ADMX, HAYSTAC (ADMX-HF)
  - QUAX
  - CASPEr-wind
  - CASPEr-Electric (EDM induced on nuclear spin)
  - ATOMIC TRANSITIONS
- **HELIOSCOPES: axion production in the Sun**
  - **CAST, Baby-IAXO**
  - **TASTE, SUMICO**
- **PURE LABORATORY EXPERIMENTS**
  - **LSW (Light Shining through Wall), PVLAS (vacuum polarization)**
  - **axion-mediated 5$^{\text{th}}$ force measurements**

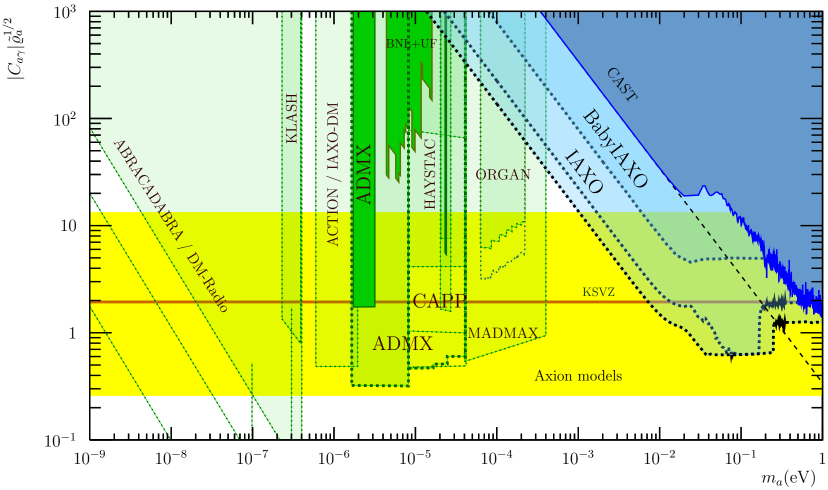

from I.G. Irastorza and J. Redondo, arXiv:1801.08127v2 [hep-ph]

AXION-ELECTRON COUPLING

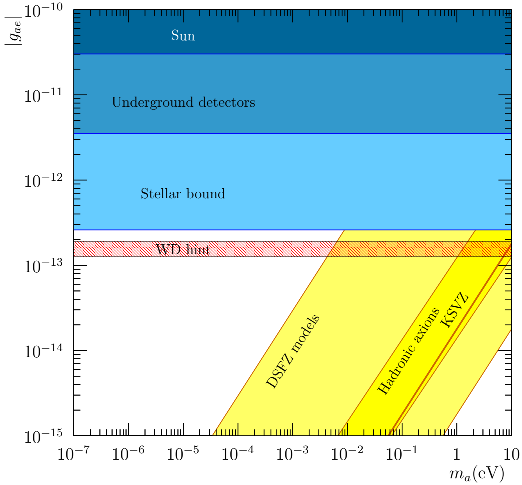

from I.G. Irastorza and J. Redondo, arXiv:1801.08127v2 [hep-ph]

ENERGY LEVEL DIAGRAM OF RE^{3+} IN $LaCl_3$

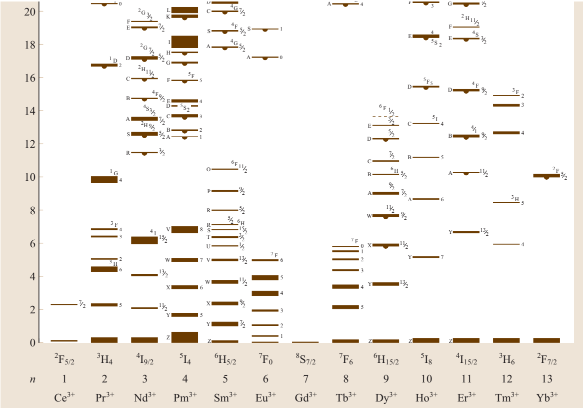

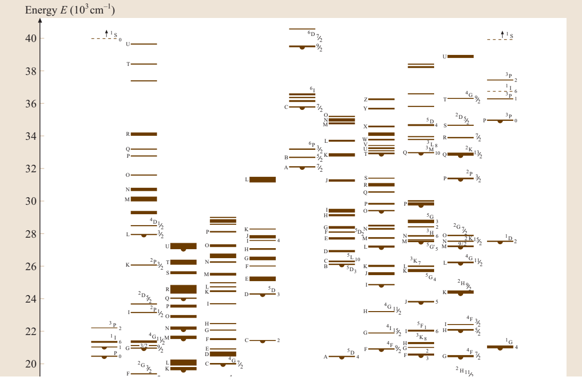

– 4f electrons
– electrostatic interaction 10^4 cm^{-1}

– further splitting by spin-orbit interaction 10^3 cm^{-1}
– crystal field (Stark splitting)

ENERGY SPLITTINGS IN RE-DOPED MATERIALS

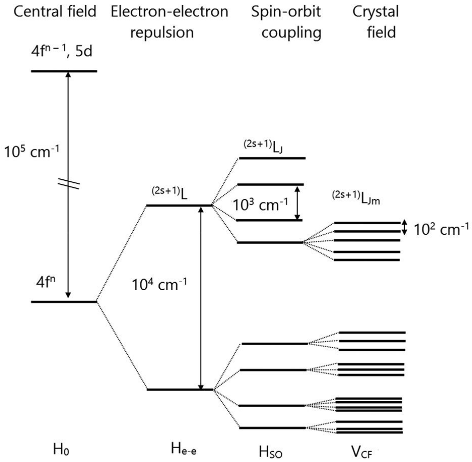

$10^4\,\mathrm{cm}^{-1} = 1.24\,\mathrm{eV}$